Available online at www.sciencedirect.com

ScienceDirect

Procedia Structural Integrity 64 (2024) 1857–1864

Structural Integrity
Procedia

www.elsevier.com/locate/procedia

SMAR 2024 – 7th International Conference on Smart Monitoring, Assessment and Rehabilitation of Civil Structures

The influence of CFRP fatigue behavior on CFRP-to-steel bonded joints

Tommaso Papa[a,*], Massimiliano Bocciarelli[a], Pierluigi Colombi[a], Angelo Savio Calabrese[a]

[a]*Department of Architecture, Built Environment and Construction Engineering, Politecnico di Milano, Milan 20133, Italy*

Abstract

The application of externally bonded CFRP reinforcements has shown its effectiveness in reducing crack growth in steel elements. However, externally bonded CFRP-to-steel joints may exhibit fatigue degradation when subjected to repeated cyclic loadings, consequently leading to cohesive debonding within the adhesive layer. Therefore, the cyclic degradation of both adhesive and the composite needs to be properly investigated.

This work presents the preliminary results of an experimental and numerical investigation on the fatigue damage behavior of CFRP and its possible influence on the load response of CFRP-to-steel bonded joint. The overall fatigue degradation of the joint under single-lap direct shear (DS) conditions is numerically modelled considering separately the damage occurring in the adhesive layer and in the composite patch. The behavior of the adhesively bonded joint is described through a cohesive zone model approach, while the composite damage behavior is described by adopting a fatigue residual stiffness model based on macroscopic stiffness degradation. Experimental results of tensile fatigue tests on rectangular CFRP coupons and of cyclic single-lap direct shear tests are presented and used for the model parameters calibration. Then, the numerical response of DS tests obtained considering the composite material either elastic or accounting for the fatigue damage is compared. The interfacial behavior maintains its role as leading failure mechanism. The introduction of the composite damage behavior shows up in a reduction of the number of cycles at failure, especially for longer fatigue lifetime, while the relative slip between the two adherends is not or slightly affected.

Keywords: Inverse analysis; CFRP-to-steel bonded joints; Fatigue; Cohesive zone model.

* Corresponding author.
E-mail address: tommaso.papa@polimi.it

10.1016/j.prostr.2024.09.240

1. Introduction

In recent years, growing attention has arisen regarding the fatigue life of existing fatigue-sensitive metallic structures. Efficient and reliable strengthening techniques are therefore needed to extend their service life. Among them, the application of externally bonded (EB) composite materials on steel structures with epoxy-based adhesives have been recognized as an effective solution in restoring loading capacity or extending fatigue life. EB Carbon Fiber Reinforced Polymers (CFRP) showed their effectiveness in fatigue strengthening thanks to their peculiar properties such as high strength to weight and stiffness to weight ratios and the durability to environmental actions (Kamruzzaman et al. (2014).

In such applications, a crucial role is represented by the behavior at the interface between the steel substrate and the composite. In fact, the interface is responsible for the load transfer between composite and substrate, mainly occurring through shear stress exchange mechanism, which is strongly affected by the properties of the structural adhesive employed (Borrie et al. (2021); Colombi et al. (2024a); Colombi and Fava (2012)). Different approaches have been developed to describe the interfacial behavior and estimating the fatigue-life. Among them, worth mentioning is the adoption of Cohesive Zone Models (CZM). In particular, the adoption of Cyclic CZM (CCZM) represents a valid and efficient approach for the numerical description of bonded interfaces between two adherends (Mohajer et al. (2020); Papa and Bocciarelli (2023); Park and Paulino (2011)).

In CFRP-to-steel bonded joints, both composite and adhesive exhibit a progressive degradation during fatigue cyclic loading (Barbosa et al (2019)). Failure usually occurs due to cohesive debonding at the interface and the cyclic degradation of the composite has been generally neglected (Doroudi et al. (2020)). Alternatively, the composite fatigue degradation has been included within the non-linear behavior of the adhesive interface (Mohabeddine et al. (2022)). Recently, the adoption of new adhesives with high performances has led to larger loads levels transferred to the composite reinforcement and higher number of loading cycles at failure can be reached. Accordingly, the effect of fatigue on the CFRP element (plate or sheet) turned out to assume a relevant role on the bonded system fatigue behavior. Different models have been proposed to describe the composite damage behavior. Among them, residual stiffness or strength models represent a valid and more practical solution (Alam et al. (2019); Degrieck and Van Paepegem (2001) for the purposes of the present study.

This work presents the preliminary results of an experimental and numerical investigation on the composite fatigue damage behavior and its influence on CFRP-to-steel bonded joints response. Tensile fatigue tests of CFRP laminate rectangular coupons are first carried out and the cyclic stiffness degradation is recorded. Then, single-lap direct shear (DS) tests have been performed to investigate the fatigue behavior of the CFRP/steel bonded joint. Finally, the global fatigue response of the system is numerically investigated considering both the damage occurring at the bonded interface and in the composite material separately by adopting a cohesive zone model and a residual stiffness model, respectively. A one-dimensional model is adopted, and the analyses have been developed with an in-house finite element solver developed in MATLAB. The obtained experimental single lap DS tests results are used to calibrate the parameters of the damage models adopted.

Nomenclature

D	composite damage variable
k	interface damage variable
E	CFRP elastic modulus
Σ	fatigue failure index
X_T	Composite static strength

2. Damage models

This section presents the numerical models adopted to describe the damage occurring at the bonded interface and in the composite material.

2.1. An exponential cohesive zone law for monotonic and cyclic loading

The damage-based cyclic cohesive zone model originally proposed in Bocciarelli (2021) for monotonic and cyclic loading is adopted in this work. The interface behavior under monotonic loading is governed by the definition of a free energy potential, with an exponentially decaying softening curve (see Figure 1a) as function of a scalar effective opening displacement, δ. The possible extension to cyclic loading conditions is performed by introducing a scalar damage variable, k, with a phenomenological rate equation governing its evolution in time, leading to a degrading stiffness and strength under cyclic loading.

The free energy potential Φ (Rose et al. (1981)) for the monotonic response reads as:

$$\Phi(\delta) = e\sigma_c\delta_c\left[1-\left(1+\frac{\delta}{\delta_c}\right)e^{-\delta/\delta_c}\right] \tag{1}$$

where σ_c represents the cohesive law traction peak, δ_c the corresponding critical displacement. From the definition in Eq. (1), the scalar measure, t^{lim}, of the effective maximum interface traction vector is computed as:

$$t^{lim} = \frac{\partial\Phi}{\partial\delta} = \frac{\sigma_c}{\delta_c}e^{(1-\delta/\delta_c)}\delta \tag{2}$$

This equation represents the monotonic bond-slip response (see Figure 1a). With η being a non-dimensional parameter coupling the normal (indicated with the subscript n) and shear (indicated with the subscript s) behaviors, the scalar effective opening displacement δ is $\delta = \sqrt{\delta_n^2 + \eta^2\delta_s^2}$. The monotonic traction-separation law reads as:

$$\begin{bmatrix} t_n^{lim} \\ t_s^{lim} \end{bmatrix} = \begin{bmatrix} \partial\Phi/\partial\delta_n \\ \partial\Phi/\partial\delta_s \end{bmatrix} = \frac{\partial\Phi}{\partial\delta}\begin{bmatrix} \partial\delta/\partial\delta_n \\ \partial\delta/\partial\delta_s \end{bmatrix} = \frac{t^{lim}}{\delta}\begin{bmatrix} \delta_n \\ \eta^2\delta_s \end{bmatrix} \tag{3}$$

where δ_n and δ_s represent the normal and shear components of the discontinuity displacement vector, respectively, and t_n^{lim} and t_s^{lim} are the maximum traction vector components transferred along the interface.
To extend this law to cyclic debonding processes, linear damaging radial paths from the origin to the maximum attainable scalar interface traction t^{lim} are assumed as per $t=F(k)\delta<t^{lim}(k)$ where F(k) is a degrading stiffness function of the damage variable k. It follows that:

$$\begin{bmatrix} t_n \\ t_s \end{bmatrix} = F(k)\begin{bmatrix} \delta_n \\ \eta^2\delta_s \end{bmatrix} \leq \begin{bmatrix} t_n^{lim} \\ t_s^{lim} \end{bmatrix} \tag{4}$$

From Eq.(2), it follows that:

$$F(k) = \frac{\sigma_c}{\delta_c}e^{(1-\tilde{\delta}(k)/\delta_c)} \tag{5}$$

where $\tilde{\delta}(k)$ is a fictitious displacement governing the evolution of the damage variable k according to:

$$k = \left[1-\left(1+\frac{\tilde{\delta}}{\delta_c}+\frac{1}{2}\left(\frac{\tilde{\delta}}{\delta_c}\right)^2\right)e^{-\tilde{\delta}/\delta_c}\right]^{\lambda} \tag{6}$$

In Eq. (6) λ is a model parameter affecting the damage evolution. This effective fictitious displacement $\tilde{\delta}(k)$ must satisfy the following conditions: equal to zero when k equal to zero and equal to ∞ when k equal to 1. The damage variable k assumes values between 0, indicating no damage, to 1, indicating complete failure. Material softening starts at point (σ_c, δ_c) and ends at complete failure with damage variable k equal to 1 and the traction value equal to 0. For λ=1, the damage k physically represents the ratio between the energy dissipated at a given interface displacement δ and the whole interface fracture energy at disposal, i.e. the area under the bond-slip law, see Bocciarelli (2021).

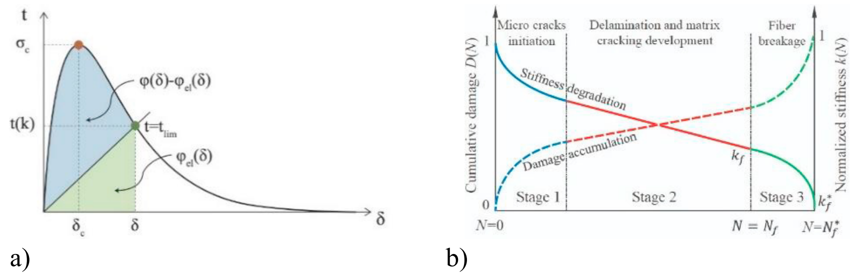

Figure 1. (a) Exponential cyclic cohesive zone law; (b) damage accumulation and stiffness degradation in the composite.

A different situation occurs during un- and re-loading cycles, fundamental to describe fatigue-driven debonding processes. For cyclic loading, the evolution of the damage parameter k is governed by the following equations:

$$\begin{cases} \dot{k} = \hat{\alpha} k[t - \beta t^{lim}(k)]\dot{\delta} \\ \dot{k} = 0 \end{cases} \quad \text{if} \quad \begin{matrix} [t - \beta t^{lim}]\dot{\delta} > 0 \\ [t - \beta t^{lim}]\dot{\delta} < 0 \end{matrix} \tag{7}$$

with $\hat{\alpha} = \alpha > 0$ for $\dot{\delta} > 0$ and $\hat{\alpha} = -\gamma < 0$ for $\dot{\delta} < 0$ and where the upper dot denotes the corresponding rate quantity.

A new set of model parameters, namely α, β and γ, is introduced in Eq. (7). These parameters, together with λ, govern the cyclic response behaviour and are then referred to as fatigue parameters. In particular, α represents the rate of damage accumulation during loading, while γ represents the rate of damage reduction (crack healing) during the un-loading cycle phase. Finally, β governs the fatigue threshold between the two above mechanisms.

According to Eq. (7), during un- and re-loading cycles the following alternatives hold:

- Initial unloading stage: $\dot{\delta} < 0$ and $t > \beta t^{lim}$; then, $[t - \beta t^{lim}]\dot{\delta} < 0$ and $\dot{k} = 0$, which means no damage evolution.
- Final unloading stage: $\dot{\delta} < 0$ and $t < \beta t^{lim}$; then, $[t - \beta t^{lim}]\dot{\delta} > 0$ and $\dot{k} = -\gamma k[t - \beta t^{lim}]\dot{\delta} < 0$, which means damage healing or crack retardation.
- Initial reloading stage: $\dot{\delta} > 0$ and $t < \beta t^{lim}$; then, $[t - \beta t^{lim}]\dot{\delta} < 0$ and $\dot{k} = 0$, which means no damage evolution.
- Final reloading stage: $\dot{\delta} > 0$ and $t > \beta t^{lim}$; then, $[t - \beta t^{lim}]\dot{\delta} > 0$ and $\dot{k} = \alpha k[t - \beta t^{lim}]\dot{\delta} > 0$, which means damage incrementation.

2.2. A residual stiffness model for composite cyclic damage

Generally, in fiber-reinforced composites fatigue damage is a quite complex phenomenon. These materials present an anisotropic and heterogeneous behavior, with different types of damage mechanisms interacting among them (Degrieck and Van Paepegem (2001)). Based on the experimental outcomes, the fatigue damage process can be divided into three main stages of stiffness degradation (Figure 1b): rapid initial decline, linear gradual reduction, and final rupture. Different fatigue failure models have been proposed in the literature and they can be classified into three main categories: fatigue life models not considering the actual degradation mechanisms but using S-N curves or Goodman-type diagrams; phenomenological models for residual stiffness or strength representation; and progressive damage models using measurable damage-related internal variables. The second class of models represents a suitable choice for the material description in this study. The phenomenological models introduce an evolution law describing the gradual degradation of stiffness or strength in terms of macroscopically observable properties, such as stiffness or strength, which can be measured during tests. In this work, a residual stiffness model originally proposed in Van Paepegem and Degrieck (2002) is adopted. It introduces a measure of the stiffness loss expressed by two different terms (initiation and propagation) and it also introduces a modified static failure criterion representing the decreasing ultimate static strength. The model is one-dimensional, considering only the longitudinal stiffness in the loading direction. The scalar damage variable D is a macroscopic index of the fatigue damage and is defined as:

$$D = 1 - \frac{E}{E_0} \tag{8}$$

where E_0 is the stiffness of the non-damaged homogenized material, while E represents the current stiffness. In this framework, the damage D evolution as function of the number of cycles N is governed by:

$$\frac{dD}{dN} = f_i(\sigma, D) + f_p(\sigma, D) \tag{9}$$

In Eq. (9), the function f_i describes the first stage of damage initiation, while f_p describes the following gradual damage propagation and final rupture. The damage initiation and damage propagation functions are:

$$f_i = c_1 \Sigma(\sigma, D) exp\left(-c_2 \frac{D}{\sqrt{\Sigma(\sigma,D)}}\right) \tag{10}$$

$$f_p = c_3 D \Sigma(\sigma, D)^2 \left[1 + exp\left(c_5(\Sigma(\sigma, D) - c_4)\right)\right] \tag{11}$$

where $\Sigma(\sigma, D)$ is the fatigue failure index, defined as 1/R, with R being the calculated safety factor from the Tsai-Wu static failure criterion:

$$\Sigma(\sigma, D) = \frac{1}{R} = \frac{\tilde{\sigma}}{X_T} = \frac{\frac{\sigma}{1-D}}{X_T} = \frac{E_0 \varepsilon}{X_T} \tag{12}$$

with ε indicating the strain and X_T the static strength, respectively, while $\tilde{\sigma}$ represents the effective stress. Eq. 12 shows that Σ expresses a ratio between the effective stress and corresponding strength.
Five different parameters are present in the model and called c_i (i=1…5). The first two affect the damage initiation phase, while the remaining three the damage propagation phase. In particular: the constant c_1 represents the damage initiation rate, while the exponential function depends on the damage D and constant c_2 associated with the saturating damage level. Moreover, c_3 represents the damage propagation rate, c_4 is a stress threshold below which no fiber fracture occurs and once this threshold is passed the exponential function increases the damage evolution very fast leading to final failure according to c_5.

3. Experimental study

This section presents the results of an experimental campaign carried out at the Material Testing Laboratory of the Politecnico di Milano, aimed at investigating the composite fatigue damage behavior and its influence on the response of bonded joints systems.

The adopted pultruded CFRP lamina has a 0.68 carbon fibre volume fraction, and the main mechanical properties are reported in Table 1, as provided by the manufacturer (Sika Italia (2019)). Specimens with a length equal to 200mm are cut from a 100mm wide composite laminate. They present a width and thickness equal to 20mm and 1.4mm, respectively. First, unidirectional tensile fatigue tests on three rectangular CFRP coupons have been carried out for the characterization of material degradation when subjected to cyclic loadings and for the subsequent model parameters calibration (see Figure 2a). Different tensile fatigue loading conditions have been considered as reported in Table 2. Specimens are initially subjected to a displacement-controlled loading ramp, until the average fatigue load is attained. After that, the control is switched to force mode and constant sinusoidal loading cycles are performed with a frequency of 6 Hz. A target number of 1 million cycles is considered. The specimens are named following the notation T_F_n, where T (tensile) indicates the test type, F indicates the loading scheme (fatigue), and n is the specimen number. The axial strain of the specimens is continuously measured during the fatigue loading using a strain gauge, 10 mm long, bonded to the specimen surface, along the load direction. The reduction of specimen elastic

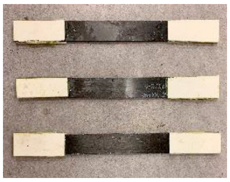

a)

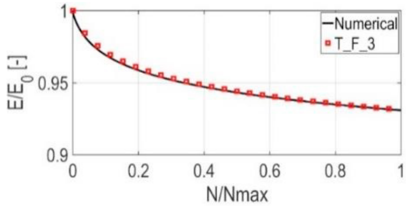

b)

Figure 2. (a) CFRP rectangular coupons; (b) comparison between experimental and numerical normalized stiffness of T_F_3 specimen.

modulus (E/E_0) is adopted as a measure of material degradation. Only for specimen T_F_1, the test was interrupted after 462×10^3 cycles because no strain accumulation neither elastic modulus reduction were detected due to the low level of fatigue loading. Similarly, the CFRP coupon T_F_2 did not show any significant degradation during the loading cycles. Specimen T_F_3, which was subjected to the highest load, showed a progressive damage evolution, although limited, which is reported in Figure 2b.

Table 1. Mechanical and geometrical properties of CFRP coupons and single-lap DS specimens.

Material	Elastic modulus E_0 [GPa]	Tensile strength [MPa]	Ultimate tensile strain [%]	Specimen orientation [°]
CFRP	190	2800	>1.80	0
Steel	210	430	15	-
Adhesive	3.65	21	1.35	-

Then, the result of one single-lap DS fatigue test is considered to investigate the fatigue behavior of the CFRP/steel bonded joint featuring the same composite material tested in tension. The specimen consisted of a CFRP lamina bonded to the flange of a HEB100 standard steel profile (S275) using a rubber-toughened epoxy adhesive (see Table 1). The specimen was tested under cyclic loading ranging between 10.07 kN and 20.13 kN, which represent the 32.5% and 70% of its quasi-static capacity, respectively. The corresponding applied load P- global slip g experimental response is shown in Figure 3a, where g represents the relative displacement between composite and substrate, measured at the loaded end using displacement transducers (LVDTs). The reader is referred to Colombi et al. (2024a) and (2024b) for further details.

Table 2. Fatigue tests on CFRP specimens.

Specimen	P_{max} [kN]	P_{min} [kN]	Load ratio [-]	N_f [x10^3]
T_F_1	20.13	10.07	0.50	462
T_F_2	47.04	36.98	0.79	1140
T_F_3	62.72	52.66	0.84	1170

4. Numerical modelling and results

This section presents the first results obtained from the numerical modelling of CFRP-to-steel bonded systems, considering the influence of the composite damage behavior. A single lap DS configuration is considered, where the substrate is conceived as rigid, while the reinforcement as linear elastic or with a damaging behavior. The interfacial behavior is modelled by zero-thickness interface elements whose non-linear response is described by the cohesive law above introduced.

The parameters of the cohesive law, controlling the static behaviour, were calibrated from the results of static single lap DS tests discussed in (Colombi et al. (2024a)). Peak shear stress τ_{max}=17.63MPa and fracture energy G_f=4.05N/mm were obtained. The fatigue parameters α=0.2483, β=0.625, γ=0.0, and λ=0.60 were identified based on the results of

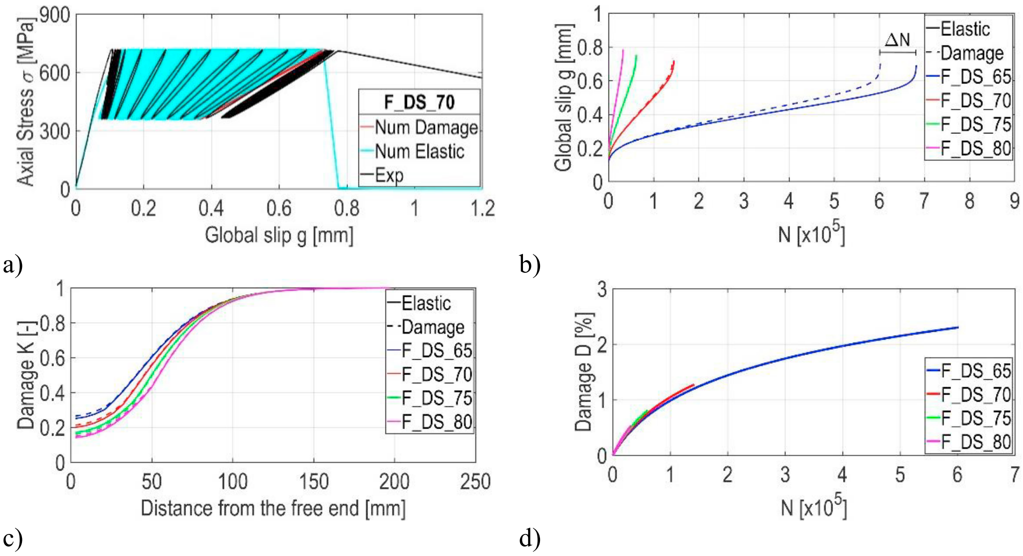

Figure 3. Comparison between elastic and damaging composite in single-lap DS tests response: (a) load-displacement curves of F_DS_70 specimen; (b) variation of displacement at the loaded end with respect to the number of cycles; (c) variation of the interface damage variable k along the bonded length at failure; (d) variation of composite damage D along the bonded length at failure.

the DS specimen tested under cyclic loading, depicted in Figure 3a (Colombi et al. (2024b)). Regarding the CFRP composite, an elastic modulus E_0=190GPa and a static strength X_T=2800MPa were adopted. As for the cyclic behaviour, the model parameters c_i were determined based on the results of specimen T_F_3 (see Figure 2b), where the variation in normalized stiffness E/E_0 with respect to the number of cycles N and the comparison between experimental and numerical curves is presented. In particular, only the first three parameters were calibrated because the rupture of the specimens did not occur and they were, namely, c_1=0.5e-05, c_2=50 and c_3=4.0e-006.

Four numerical analyses were conducted on the same direct shear model, corresponding to four different amplitude of the maximum fatigue load, namely: 65%, 70%, 75% and 80% of the joint static capacity. The load ratio was maintained equal to 0.5. The analyses are named following the notation DS_F_%, where DS (=direct shear) indicates the test setup, F indicates the loading scheme (fatigue) and % indicates the percentage of maximum applied load with respect the static capacity. For each analysis, two numerical responses were obtained, considering the CFRP composite either elastic or accounting for the fatigue damage. In the latter case, the damage occurring in the composite material was considered separately from that involving the bonded interface, according to the non-linear models adopted, i.e., residual stiffness model and cyclic CZM.

Figure 3a shows the numerical load-global slip curves of analysis DS_F_70, including the response associated with the CFRP composite elastic behaviour (labelled “Num Elastic” in Figure 3a) and that corresponding with the exponential damage behavior (labelled “Num Damage” in Figure 3a). As can be noted, the introduction of the composite damage behaviour does not influence significantly the global slip of the joint. However, the same ultimate global slip is reached with a lower number of cycles. This behavior was more evident when a higher number of cycles was achieved (i.e. when maximum fatigue load was lower), as evidenced by the term ΔN corresponding to approximately 10% for analysis DS_F_65 in Figure 3b where the variation of the global slip with respect to the number of cycles is reported. Figure 3c show the variation of the cohesive interface damage variables k, computed at the last step before failure along the bonded length. The difference between the two assumptions (composite either elastic or damaging) turns out to be negligible, showing that the interfacial damage behaviour remains dominant and that its variation is not significantly influenced by damage in the composite material. Figure 3d shows the variation of the composite damage with the number of cycles. The four curves show a different trend with an increasing gradient with the increase of the load level accompanied by a reduction of the cycles sustained. Therefore, composite damage reduces the number of cycles at failure, when the load level applied is lower, because this implies a higher number of cycles at failure and, therefore, a larger damage can be developed in the composite.

5. Conclusions

In this work, preliminary results of an experimental and numerical investigation on the bond response of EB CFRP-to-steel systems were presented. Tensile fatigue tests on CFRP specimens were first conducted to investigate composite damage behavior and calibrate the parameters of a residual stiffness model. Single-lap DS tests were then considered with the adoption of an exponential bond-slip cohesive model to represent the adhesive behavior. Then, damage in the composite and at the interface was considered separately. The different behaviour of DS tests between the two assumptions, i.e., with composite material either elastic or with a damaging behavior, was numerically investigated.

Based on these first results, the adoption of the proposed residual stiffness model resulted to be suitable in describing the composite response for this study. As bonded joints, the numerical results highlighted the influence of the composite damage on the number of cycles at failure, rather than on the ultimate displacement which seems to be not or slightly influenced. Possible future studies could investigate the influence of various parameters involved. Such as the stress ratio, size effect, fiber orientation, and others.

Acknowledgements

The support of the Politecnico di Milano is gratefully acknowledged.

References

Alam, P., Mamalis, D., Robert, C., Floreani, C., Ó Brádaigh, C.M., 2019. The Fatigue of Carbon Fibre Reinforced Plastics - A Review. Composites Part B: Engineering 166:555–79. doi: 10.1016/j.compositesb.2019.02.016

Bocciarelli, M., 2021. A New Cohesive Law for the Simulation of Crack Propagation under Cyclic Loading. Application to Steel- and Concrete-FRP Bonded Interface. Theoretical and Applied Fracture Mechanics 114. doi: 10.1016/j.tafmec.2021.102992.

Barbosa, J., Correia, J.A.F.O., Júnior, RCS F., Zhu, S-P., De Jesus, A.M.P., 2019. Probabilistic S-N fields based on statistical distributions applied to metallic and composite materials: State of the art. Advances in Mechanical Engineering. 11. doi:10.1177/1687814019870395.

Borrie, D., Al‐saadi, S., Zhao, X.L., Singh Raman, R.K., Bai, Y., 2021. Bonded Cfrp/Steel Systems, Remedies of Bond Degradation and Behaviour of CFRP Repaired Steel: An Overview. Polymers 13(9). doi: 10.3390/polym13091533

Colombi, P., Bocciarelli, M., Calabrese, A.S., D'antino, T., Papa, T., 2024a. Externally Bonded CFRP Reinforcement of Steel Structures: Mechanical Characterization of a Toughened Epoxy Adhesive. 6th International Conference on Smart Monitoring, Assessment and Rehabilitation of Civil Structures, SMAR 2022. Shanghai, China, Vol. 259: 625 - 637. doi: 10.1007/978-981-99-3362-4_50

Colombi, P., Bocciarelli, M., Calabrese, A.S., D'Antino, T., Papa, T., 2024b. Application of a Toughened Epoxy Adhesive for the Fatigue Strengthening of Steel Structures. 6th International Conference on Smart Monitoring, Assessment and Rehabilitation of Civil Structures, SMAR 2022. Shanghai, China, Vol. 259: 639 - 651. doi: 10.1007/978-981-99-3362-4_51

Colombi, P., Fava., G., 2012. Fatigue Behaviour of Tensile Steel/CFRP Joints. Composite Structures 94(8):2407–17. doi: 10.1016/j.compstruct.2012.03.001.

Degrieck, J., Van Paepegem. W., 2001. Fatigue Damage Modelling of Fibre-Reinforced Composite Materials. Vol. 54. doi: 10.1115/1.1381395

Doroudi, Y., Fernando, D., Zhou, H., Nguyen, V.T., Ghafoori, E., 2020. Fatigue Behavior of FRP-to-Steel Bonded Interface: An Experimental Study with a Damage Plasticity Model. International Journal of Fatigue 139. doi: 10.1016/j.ijfatigue.2020.105785.

Kamruzzaman, M., Jumaat, M.Z., Ramli Sulong, N. H., Saiful Islam, A. B. M., 2014. A Review on Strengthening Steel Beams Using FRP under Fatigue. Scientific World Journal 2014. doi: 10.1155/2014/702537.

Mohabeddine, A., Correia, J., Montenegro, P.A., De Jesus, A., Castro, J.M., Calçada, R., Berto, F., 2022. An Approach for Predicting Fatigue Life of CFRP Retrofitted Metallic Structural Details. International Journal of Fatigue 154. doi: 10.1016/j.ijfatigue.2021.106557.

Mohajer, M., Bocciarelli, M., Colombi, P., Hosseini, A., Nussbaumer, A., Ghafoori, E., 2020. Irreversible Cyclic Cohesive Zone Model for Prediction of Mode I Fatigue Crack Growth in CFRP-Strengthened Steel Plates. Theoretical and Applied Fracture Mechanics 110:102804. doi: 10.1016/j.tafmec.2020.102804.

Papa, T., Bocciarelli, M., 2023. Identification of the Parameters Contained in a Cyclic Cohesive Zone Model for Fatigue Crack Propagation. Engineering Fracture Mechanics 279. doi: 10.1016/j.engfracmech.2023.109055.

Park, K., Paulino, G.H., 2011. Cohesive Zone Models: A Critical Review of Traction-Separation Relationships across Fracture Surfaces. Applied Mechanics Reviews 64(6). doi: 10.1115/1.4023110.

Rose, J. H., Ferrante, J., Smith, J.R., 1981. Universal Binding Energy Curves for Metals and Bimetallic Interfaces. Physical Review Letters 47(9):675–78. doi: 10.1103/PhysRevLett.47.675.

Sika Italia S.p.A. Sika CarboDur M614(IT) Scheda Dati Prodotto 2019.

Van Paepegem, W., Degrieck, J., 2002. A New Coupled Approach of Residual Stiffness and Strength for Fatigue of Fibre-Reinforced Composites. Vol. 24. doi: 10.1016/S0142-1123(01)00194-3